Astronomy
&
Astrophysics

Local models of stellar convection

II. Rotation dependence of the mixing length relations

P. J. Käpylä[1,2], M. J. Korpi[3], M. Stix[2], and I. Tuominen[1,4]

[1] Astronomy Division, Department of Physical Sciences, PO Box 3000, 90014 University of Oulu, Finland
   e-mail: petri.kapyla@oulu.fi
[2] Kiepenheuer–Institut für Sonnenphysik, Schöneckstrasse 6, 79104 Freiburg, Germany
[3] NORDITA, Blegdamsvej 17, 2100 Copenhagen, Denmark
[4] Observatory, PO Box 14, 00014 University of Helsinki, Finland

Abstract. We study the mixing length concept in comparison to three-dimensional numerical calculations of convection with rotation. In a limited range, the velocity and temperature fluctuations are linearly proportional to the superadiabaticity, as predicted by the mixing length concept and in accordance with published results. The effects of rotation are investigated by varying the Coriolis number, Co $= 2\Omega\tau$, from zero to roughly ten, and by calculating models at different latitudes. We find that α decreases monotonically as a function of the Coriolis number. This can be explained by the decreased spatial scale of convection and the diminished efficiency of the convective energy transport, the latter of which leads to a large increase of the superadiabaticity, $\delta = \nabla - \nabla_{ad}$ as function of Co. Applying a decreased mixing length parameter in a solar model yields very small differences in comparison to the standard model within the convection zone. The main difference is the reduction of the overshooting depth, and thus the depth of the convection zone, when a non-local version of the mixing length concept is used. Reduction of α by a factor of roughly 2.5 is sufficient to reconcile the difference between the model and helioseismic results. The numerical results indicate reduction of α by this order of magnitude.

Key words. hydrodynamics – Sun: interior – convection – star: evolution

1. Introduction

The mixing length concept was originally developed to deal with terrestrial incompressible convection (e.g. Taylor 1915; Prandtl 1925). Later, this approach was adopted in the context of stellar convection (Biermann 1932; Cowling 1935), and the version introduced by Vitense (1953, see also Böhm-Vitense 1958) is still the most widely used description for convection in stellar structure models. The main advantage of this model is its simplicity; only one fixed free parameter is needed which relates the correlation length to the local pressure scale height. In stellar structure and evolution models the mixing length parameter, α, is needed in order to determine the temperature gradient in the convection zone. The value of α fixes the depth of the convection zone in the model, which, for the solar case, is known from helioseismology (e.g. Monteiro et al. 1994; Christensen-Dalsgaard et al. 1995).

Despite the crude nature of the mixing length concept, it can be useful in the bulk of the solar convection zone due to the fact that the temperature gradient there is nearly adiabatic, and the actual description of convection does not make much difference.

One way to test the validity of the mixing length concept is to perform numerical calculations of convection. Comparisons have been done e.g. by Chan & Sofia (1987, 1989), Kim et al. (1996), and Porter & Woodward (2000). The main result of these studies is that the relations derived between various mean thermodynamic and kinematic quantities under the basic mixing length assumption are good approximations when the superadiabaticity, $\delta = \nabla - \nabla_{ad}$, is small enough (Kim et al. conclude that it is sufficient to have $\delta \leq 0.01$). Interestingly, Chan & Sofia (1987) find that the basic mixing length assumption, $l = \alpha H_p$, is realised in their model.

The mixing length concept, and the aforementioned comparisons to numerical convection, all neglect the effects of rotation, which can be dynamically important in many stars with convective envelopes. For example, the mixing length models of the solar convection zone (e.g. Stix 2002) yield velocities of the order of 10 m s^{-1} near the bottom of the convection zone. Furthermore, assuming the approximate size of the convective elements to be of the order of the pressure scale height ($H_p \approx 5 \times 10^7$ m), one can estimate the turnover time to be $\tau \approx 10^6$ s. The solar angular velocity is $\Omega_\odot \approx 2.6 \times 10^{-6}$ s^{-1}, with which one can estimate the Coriolis number, Co $= 2\Omega\tau$,

to be of order ten near the bottom of the convection zone and of order unity in a large fraction of the convection zone (Fig. 1).

We present three-dimensional calculations of convection in a rectangular domain that represents a small portion of a full star at some latitude. The latitude of the box can be chosen by imposing a suitably oriented rotation vector. In the present paper, our main aim is to parametrise the effects of rotation on the mixing length α. This is achieved by calculating several boxes with varying rotational influence and latitude. One can think of the variation of the Coriolis number as the variation of the radial position in a convection zone. Thus, we obtain a radial profile for the mixing length α which we introduce into a solar model.

In Sect. 2 of this paper the computational model is described, and in Sect. 3 a short summary of the mixing length concept is given. In Sects. 4 and 5 we discuss the parameter ranges of the calculations and summarise the results.

2. The model

A description of the model setup can be found in Käpylä et al. (2004; hereafter Paper I), and that of the numerical method in Caunt & Korpi (2001). The computational domain is a rectangular box, situated at a latitude Θ. The coordinates are chosen so that x, y, and z correspond to the south-north, west-east, and radially inward directions, respectively. The angular velocity as function of latitude is $\mathbf{\Omega} = \Omega(\cos\Theta\hat{e}_x - \sin\Theta\hat{e}_z)$.

The gas is assumed to obey the ideal gas equation

$$p = \rho e(\gamma - 1), \tag{1}$$

where $\gamma = c_P/c_V = 5/3$ is the ratio of the specific heats.

To model the radiative losses near the surface we use a narrow cooling layer on the top of the convection zone, cooled with a term

$$\Gamma_{\text{cool}} = \frac{1}{t_{\text{cool}}} f(z)(e - e_0), \tag{2}$$

where t_{cool} is a cooling time, chosen to be short enough for the upper boundary to stay isothermal, $f(z)$ a function which vanishes everywhere else but in the interval $z_0 \leq z < z_1$, and $e_0 = e(z_0)$ the value of internal energy at the top of the box.

We adopt periodic boundary conditions in the horizontal directions, and closed stress free boundaries at the top and bottom. The temperature is kept fixed at the top of the box and a constant heat flux is applied at the bottom

$$\frac{\partial u_x}{\partial z} = \frac{\partial u_y}{\partial z} = u_z = 0 \qquad \text{at} \quad z = z_0, z_3; \tag{3}$$

$$e(z_0) = e_0, \tag{4}$$

$$\left.\frac{\partial e}{\partial z}\right|_{z_3} = \frac{g}{(\gamma - 1)(m_3 + 1)}, \tag{5}$$

where m_3 is the polytropic index in the lower overshoot layer.

We obtain nondimensional quantities by setting

$$d = \rho_0 = g = c_P = 1.$$

Thus, length is measured with respect to the depth of the unstable layer, $d = z_2 - z_1$, and density in units of the initial value
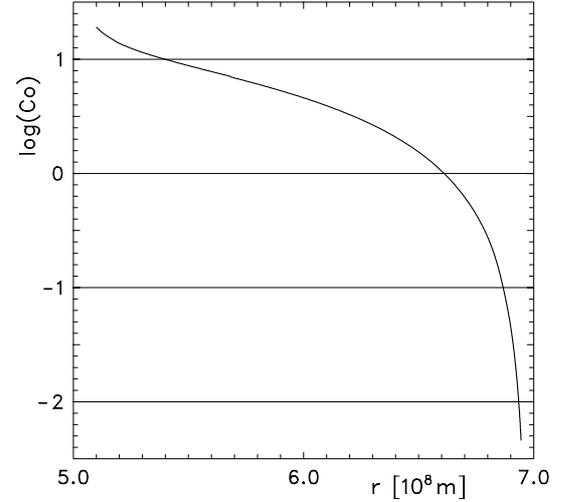

Fig. 1. Logarithm of the Coriolis number, $\text{Co} = 2\Omega_\odot \alpha H_p/v$, in the solar convection zone.

at the bottom of the convectively unstable layer, ρ_0. Time is measured in units of the free fall time, $\sqrt{d/g}$, velocity in units of $\sqrt{dg}$, and entropy in terms of c_P. The box has horizontal dimensions $L_x = L_y = 4$, and $L_z = 2$ in the vertical direction. The upper boundary is situated at $z_0 = -0.15$ and the upper boundary of the convectively unstable layer is at $z_1 = 0$. The lower boundaries of the unstable layer and of the lower stably stratified region are at $(z_2, z_3) = (1, 1.85)$, respectively.

The dimensionless parameters controlling the calculations are the Prandtl number Pr, and the Taylor and Rayleigh numbers, denoted by Ta and Ra, respectively. The relative importance of thermal diffusion against the kinetic one is measured by the Prandtl number

$$\text{Pr} = \frac{\nu}{\chi_0}, \tag{6}$$

where χ_0 is the reference value of the thermal diffusivity, taken from the middle of the unstably stratified layer. In the present study, ν is a constant. We set $\text{Pr} = 0.4$ which is a compromise between computational time (large diffusivity enforces a smaller time step) and realistic physics (in the Sun $\text{Pr} \ll 1$).

Rotation is measured by the Taylor number

$$\text{Ta} = \left(\frac{2\Omega d^2}{\nu}\right)^2. \tag{7}$$

A related dimensionless quantity is the Coriolis number, which is the inverse of the Rossby number, $\text{Co} = 2\Omega\tau$, where $\tau = d/u_t$ is the convective turnover time, and u_t the rms-value of the fluctuating velocity determined through the calculation and averaged over the convectively unstable layer and time. In our calculations Co varies by about two orders of magnitude from about 0.1 to roughly 14.

Convection efficiency is measured by the Rayleigh number

$$\text{Ra} = \frac{d^4 g\delta}{\chi_0 \nu H_p}, \tag{8}$$

where $\delta = \nabla - \nabla_{\text{ad}}$ is the superadiabaticity, measured as the difference between the actual and adiabatic logarithmic

temperature gradients, and H_p the pressure scale height, both evaluated in the middle of the unstably stratified layer in the non-convecting hydrostatic reference solution.

We define the Reynolds number as

$$\mathrm{Re} = \frac{u_t d}{\nu}. \tag{9}$$

The initial stratification is polytropic, described by the indices m_1, m_2, and m_3 for the three layers. We set $m_1 = \infty$, $m_2 = 1$, and $m_3 = 3$, respectively, which means that the cooling layer is initially isothermal, and the stratification of the lower overshoot layer resembles that of the solar model of Stix (2002).

Initially the radiative flux, $F_{\mathrm{rad}} = \kappa \nabla e$, where $\kappa = \gamma \rho \chi$ is the thermal conductivity, carries all of the energy through the domain. This constraint defines the thermal conductivities in each layer as

$$\frac{\kappa_i}{\kappa_j} = \frac{m_i + 1}{m_j + 1}. \tag{10}$$

In the calculations the vertical profile of κ is kept constant, which with the boundary condition for the internal energy, Eq. (5), assures that the heat flux into the domain is constant at all times. The initial state is perturbed with small scale velocity fluctuations of the order of $10^{-2} \sqrt{dg}$ which are deposited in the convectively unstable layer.

The code is parallelised using message passing interface (MPI). The calculations were carried out on the IBM eServer Cluster 1600 supercomputer hosted by CSC Scientific Computing Ltd., in Espoo, Finland, and on the KABUL and BAGDAD Beowulf clusters with 16 and 34 processors, respectively, at the Kiepenheuer-Institut für Sonnenphysik, Freiburg, Germany.

3. The mixing length concept

The basic assumption in the mixing length concept is that the rising and descending convective elements preserve their identity for a length which is proportional to the local pressure scale height, i.e.

$$l = \alpha H_p \tag{11}$$

where $H_p = \left(\frac{1}{p} \frac{\partial p}{\partial z} \right)^{-1}$. Using this assumption it is possible to derive equations for the mean convective velocity and temperature fluctuation (e.g. Stix 2002)

$$\langle u_z'^2 \rangle = \frac{\alpha_u^2 H_p g}{8} (\nabla - \nabla_{\mathrm{ad}}), \tag{12}$$

$$\left\langle \sqrt{T'^2} \right\rangle = \frac{\alpha_T}{2} (\nabla - \nabla_{\mathrm{ad}}) \langle T \rangle, \tag{13}$$

where adiabatic variation of the convective eddies has been assumed, and the brackets denote horizontal and temporal averaging.

The mixing length parameter enters the stellar evolution models in the context of energy transport. Thus, we relate the fluxes of enthalpy and kinetic energy with the additional equations (e.g. Porter & Woodward 2000)

$$F_e = \alpha_e c_p \langle \rho \rangle \left\langle \sqrt{T'^2} \right\rangle \left\langle \sqrt{u_z'^2} \right\rangle, \tag{14}$$

$$F_{\mathrm{kin}} = \alpha_k \langle \rho \rangle \left\langle \sqrt{u_z'^2} \right\rangle^{3/2}, \tag{15}$$

Table 1. Summary of the convection calculations.

Run	Ra	Re	Ta	Co	Θ	Grid
Co0	2.5×10^5	140	0	0	–	64^3
Co01-00	2.5×10^5	140	203	0.10	$0°$	64^3
Co01-30	2.5×10^5	140	203	0.10	$-30°$	64^3
Co01-60	2.5×10^5	138	203	0.10	$-60°$	64^3
Co01-90	2.5×10^5	138	203	0.10	$-90°$	64^3
Co1-00	2.5×10^5	139	2.03×10^4	1.04	$0°$	64^3
Co1-30	2.5×10^5	145	2.03×10^4	1.00	$-30°$	64^3
Co1-60	2.5×10^5	141	2.03×10^4	1.03	$-60°$	64^3
Co1-90	2.5×10^5	139	2.03×10^4	1.05	$-90°$	64^3
Co10-00	2.5×10^5	337	2.03×10^6	4.24	$0°$	$96^2 \times 64$
Co10-30	2.5×10^5	121	2.03×10^6	11.8	$-30°$	$96^2 \times 64$
Co10-60	2.5×10^5	105	2.03×10^6	13.6	$-60°$	$96^2 \times 64$
Co10-90	2.5×10^5	104	2.03×10^6	13.7	$-90°$	$96^2 \times 64$
s1Co0	3.1×10^5	116	0	0	–	64^3
s2Co0	1.1×10^6	250	0	0	–	128^3
s2Co01-90	1.1×10^6	256	650	0.10	$-90°$	128^3
s2Co1-00	1.1×10^6	259	6.5×10^4	1.00	$0°$	128^3
s2Co1-30	1.1×10^6	265	6.5×10^4	0.98	$-30°$	128^3
s2Co1-60	1.1×10^6	262	6.5×10^4	1.00	$-60°$	128^3
s2Co1-90	1.1×10^6	263	6.5×10^4	1.00	$-90°$	128^3
s2Co10-90	1.1×10^6	221	6.5×10^6	12.4	$-90°$	128^3
s3Co0	1.8×10^6	340	0	0	–	192^3
s4Co0	4.1×10^6	609	0	0	–	256^3

where $F_e = \langle c_p \rho T' u_z' \rangle$ and $F_{\mathrm{kin}} = \langle \frac{1}{2} \rho u^2 u_z' \rangle$ are the enthalpy and kinetic energy fluxes, respectively. We use subscripts u, T, e, and k for the mixing length parameters obtained from the relations (12) to (15) due to the fact that it is not a priori clear that all of them would yield the same value.

4. Parameter ranges in the Sun and in the calculations

4.1. Coriolis number in the Sun

The Coriolis number varies strongly in the outer convection zone of the Sun. Near the surface it is only of order 10^{-3} or smaller, but it exceeds 10 in the deeper region. Figure 1 shows Co for a standard solar model, calculated according to $\mathrm{Co} = 2\Omega l/v$, where $l = \alpha H_p$ is the mixing length, and v is the convection velocity that is obtained by means of the local mixing-length formalism. The coefficient $\alpha = 1.66$ is obtained through a calibration of a model of age 4.57×10^9 years to the present Sun.
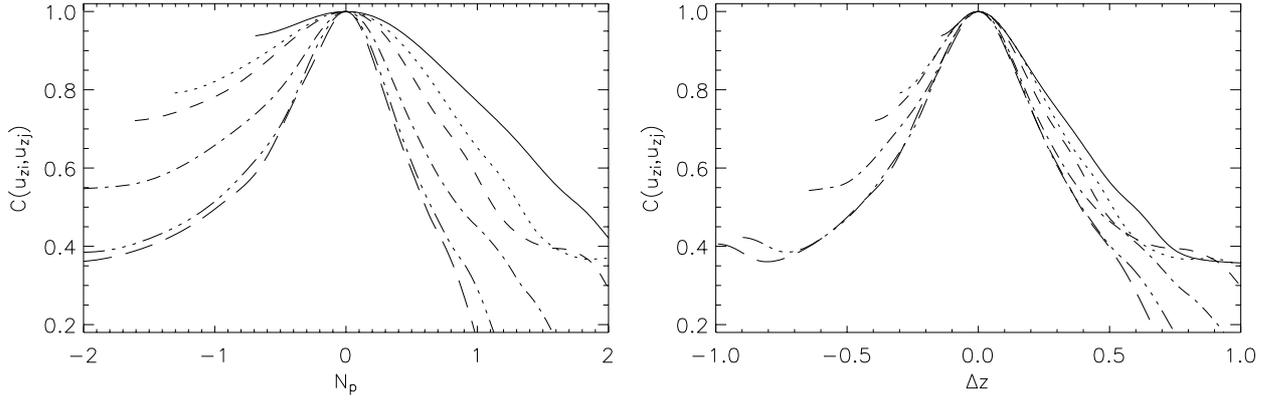
Fig. 2. Correlations of u_z with respect to the reference levels $z_{ref} = 0$ (solid), 0.17 (dotted), 0.26 (dashed), 0.5 (dot-dashed), 0.77 (triple dot dashed), and 0.87 (long dashed) from the run s2Co0 as function of the number of pressure scale heights, N_p, (*left*) and the actual distance Δz (*right*).
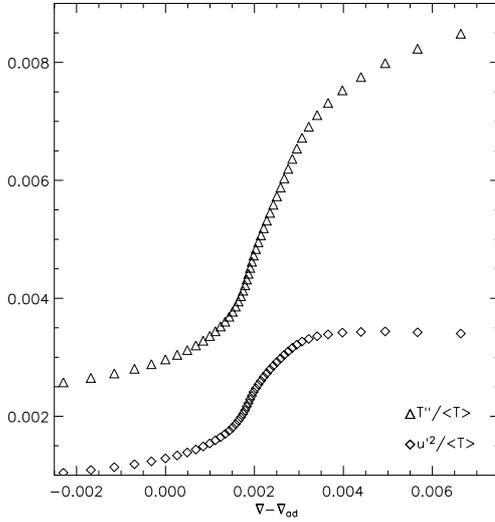

Fig. 3. Relations between the vertical velocity and temperature fluctuations versus the superadiabatic gradient from the run s2Co1-90.

4.2. Summary of the calculations

Table 1 gives a summary of the calculations. Bearing in mind the result presented in Fig. 1, we have made calculations with four different Taylor numbers, which roughly correspond to Coriolis numbers 0, 0.1, 1, and 10. We refer to these runs with a prefix Co0, Co01, Co1, and Co10, respectively. If we interpret the Coriolis number as the depth dependence, the two first cases represent roughly the top, and the latter two the middle and the bottom of the solar convection zone. To investigate the latitudinal dependence we have made calculations at four latitudes, namely $\Theta = 0°$ (equator), $-30°$, $-60°$, and $-90°$ (southern pole). In the standard setup the essentially step-function form of the thermal conductivity profile, see Eq. (10), introduces a peak in the superadiabaticity at the bottom of the convection zone (not shown). We find this feature to persist in calculations where the resolution is doubled from the values listed in Table 1 using runs from Paper I.

Thus we introduce a setup in which the logarithmic temperature gradient in the lower overshoot layer in the initial state

follows a profile

$$\nabla = \nabla_3 + \frac{1}{2}\{\tanh[4(z_m - z)] + 1\}\Delta\nabla, \tag{16}$$

where ∇_3 is the applied gradient at the bottom, and $\Delta\nabla$ the difference between the gradient in the unstable layer and the applied gradient, and z_m inflection point of the tanh-function, calculated so that $\nabla = \nabla_{ad}$ at the interface between the stable and unstable layers. The thermal conductivity is determined so that initially radiative diffusion transports the total energy flux. We denote runs with this setup by a prefix s and a number which depends on the used resolution in Table 1.

5. Results

5.1. Basic mixing length assumption

We test the basic mixing length assumption by calculating the correlation of the horizontally averaged vertical velocity as function of depth as suggested by Chan & Sofia (1987, 1989)

$$C[u_{z_{ref}}, u_z] = \frac{\langle u_{z_{ref}} u_z \rangle}{\langle u_{z_{ref}}^2 \rangle^{1/2} \langle u_z^2 \rangle^{1/2}}, \tag{17}$$

where z_{ref} is the reference level and z runs from z_0 to z_3. It is useful to plot this quantity as a function of the number of pressure scale heights

$$N_p = \Delta \ln\langle p \rangle, \tag{18}$$

where the difference is calculated from the reference level. If the basic mixing length assumption, defined by Eq. (11), is correct the correlations plotted as functions of N_p with respect to different reference levels should fall on top of each other. Figure 2 shows the correlations in the run s2Co0 case as functions of N_p and the distance measured in terms of d. The widths of the correlations measured as function of pressure scale heights decrease monotonically as a function of depth. We find that this width is more or less constant when measured in terms of d, the unit length. This result resembles the one by Robinson et al. (2003), who present calculations of convection representing the highly superadiabatic near-surface layers of the Sun.
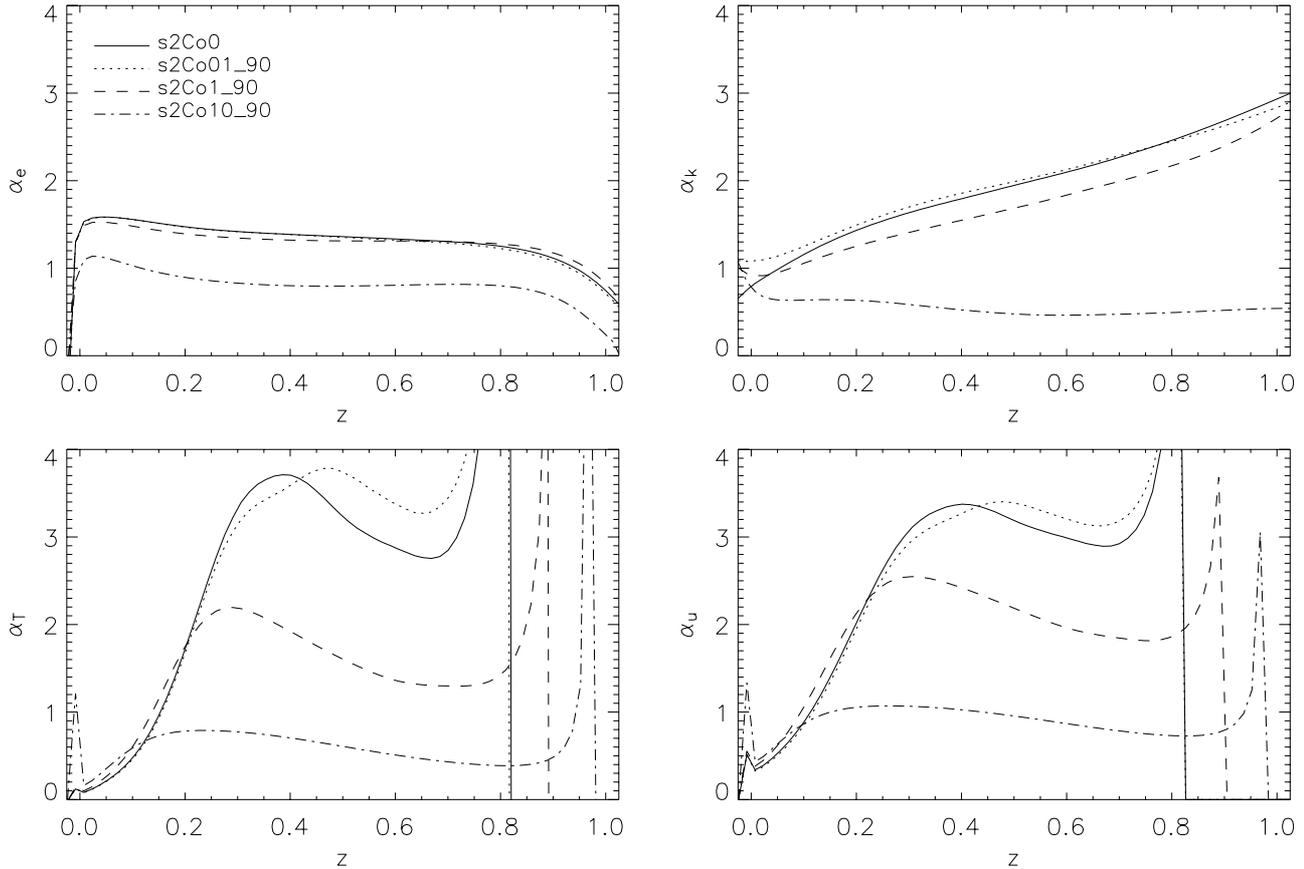
Fig. 4. The mixing length parameters calculated from Eqs. (12) to (15) as functions of depth and rotation.

Although we do not find a scaling of the correlation width with the scale height reported by Chan & Sofia (1987, 1989), we do find that the velocity and temperature fluctuations follow a more or less linear relation as function of the superadiabaticity, δ, for a limited range of parameters (see Figs. 3 and 4). This is realised in in the calculations where δ decreases monotonically within the convectively unstable region due to the more smoothly varying thermal conductivity (Figs. 5 and 7).

The linear part in Figs. 3 and 4 is clearly shorter than in the results of Chan & Sofia (1987, 1989, 1996) which can be explained by the fact that whereas in our calculations the convectively unstable region contains roughly two pressure scale-heights, Chan & Sofia typically have five or more. Our failure to find any such linear relation for the standard models is most probably due to an unrealistic step function like thermal conductivity profile which somewhat distorts the thermal structure. However, the qualitative trends seen as function of rotation do not depend on the choice of the thermal conductivity profile.

5.2. Effect of rotation and dependence on latitude

Figure 4 shows the mixing length parameters, as defined by Eqs. (12) to (15), from the s2 runs with four Coriolis numbers at latitude $-90°$. These figures show that we do not find one universal parameter α that could describe all the quantities in Eqs. (12) to (15). Firstly, α_e describing the convective energy transport, seems to have a rather well-defined value of about 1.5 for all cases bar the runs with largest rotation.

Similarly, α_k stays fairly constant for slow rotation, and shows a large reduction for the Co10 case. On the other hand, α_T and α_u decrease rapidly as Co grows. The explanation to this behaviour is that the superadiabaticity, which appears in the denominator in the equations for α_T and α_u, increases rapidly as a function of rotation (see Fig. 5). This growth of $\nabla - \nabla_{ad}$ is linked to the decrease of the convective energy transport as a function of rotation (see Paper I). The reduced convective flux forces the radiative diffusion to transport more energy, which can only be achieved by steepening the temperature gradient. However, due to the fact that the present numerical model deals with inefficient convection, where maximally about one third of the total energy flux is transported by convection, the rotational influence on the superadiabaticity is probably underestimated in comparison to the solar case where convection is expected to transport practically all energy. Preliminary numerical results with an efficient convection setup support this conjecture.

Figure 6 shows the superadiabaticity in the overshoot layer from the s2 set of calculations. The increasing effect of rotation is seen in the larger magnitude of the superadiabaticity and a significantly deeper superadiabatic layer. Furthermore, as the overshooting decreases as a function of rotation the transition at the unstable/stable interface becomes steeper due to the larger δ in the convectively unstable layer. The quantitative change of δ in the depth of the superadiabatic layer is probably exaggerated due to the much larger energy flux in the present calculations in comparison to the Sun. A similar issue concerns the transition from the overshoot to the radiative layer noted by
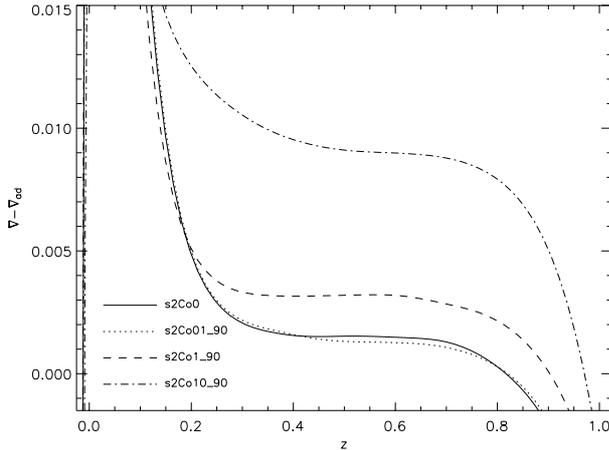
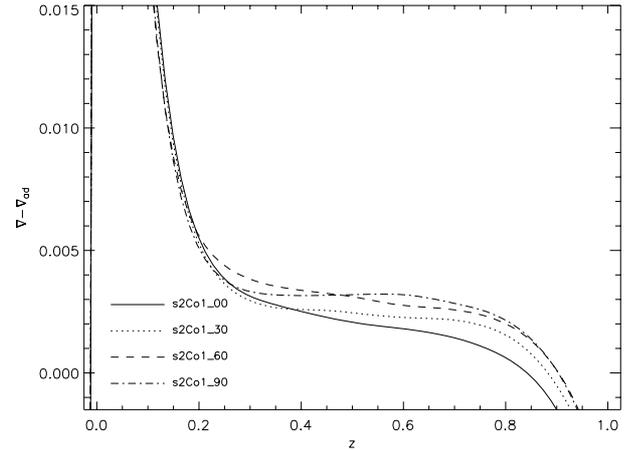**Fig. 5.** Superadiabaticity $\nabla - \nabla_{ad}$ as function of depth and rotation.

Fig. 7. Superadiabaticity $\nabla - \nabla_{ad}$ as function of depth and latitude.

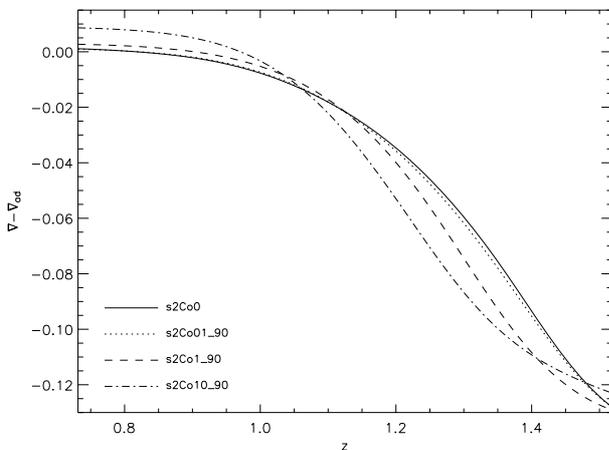**Fig. 6.** Superadiabaticity $\nabla - \nabla_{ad}$ as a function of depth and rotation in the transition layer between the convectively unstable and stable regions. Note that the scale is different by roughly an order of magnitude in comparison to Fig. 5.

Rempel (2004). According to that study, reducing the input flux sufficiently one should reach a regime where the overshoot resembles that obtained by non-local mixing length models, i.e. almost adiabatic overshoot and a sharp transition to the radiative gradient. However, this may require the use of an anelastic code due to the timestep requirement.

The main feature of the latitudinal dependence is that the superadiabaticity increases as function of latitude (see Fig. 7). Note that whereas the superadiabatic region extends as the latitude increases, the overshooting depth decreases in a similar fashion to Fig. 6. In an earlier study with denser latitude coverage (Paper I) some indications of a maximum of δ at latitudes $\Theta \approx -60° \ldots -75°$ was observed. What this implies is that convection is more efficient at low latitudes and that due to this one would expect overshooting to peak there. This is indeed observed for slow and moderate rotation, i.e. Co < 4, see Fig. 9 of Paper I. This could mean that the overshooting extends deeper at equatorial regions, which can lead to a prolate shape of the tachocline as indicated by helioseismology (Basu & Antia 2001). However, one must bear in mind that the helioseismology results refer to the shear layer whose connection with overshooting is not yet known. The thermal stratification

of the Sun does not vary observably as a function of latitude as in the numerical models which is most likely due to the much too vigorous convection in the calculation. Furthermore, we note that the trend in the overshooting depth as function of latitude seems to reverse for more rapid rotation (Paper I).

We feel that further study, beyond of the scope the present paper, of the details of the overshooting as functions of rotation and input energy flux is needed in order to determine whether it is possible to approach the mixing length regime with 3D calculations and to fully substantiate the effects of rotation which are virtually always neglected in overshooting models.

5.3. Effects of resolution

In order to study the dependence of the mixing length relations on resolution, we have made a set of runs where we vary the Rayleigh number from 3.1×10^5 to 4.1×10^6 and the number of gridpoints from 64^3 to 256^3, named s1Co0 to s4Co0 in Table 1. Figure 8 shows the mixing length parameters from the runs s1Co0 to s4Co0. The main feature of the results is that the qualitative character of the α-parameters remains unaffected when resolution changes. The relatively large changes in the parameters α_T and α_u are mostly explained by the smaller superadiabaticity as resolution increases.

The largest resolution calculation, however, is not fully comparable to the lower resolution ones due to the fact that the calculation did not reach a thermally saturated state. This has to do with the fact that in order to avoid the long thermal relaxation phase we start the calculation with a stratification that is expected to be close to the final thermally relaxed state. This procedure has to be carried out by trial and error for each resolution and for the 256^3 run the initial guess of the stratification was too superadiabatic, resulting in too efficient convection. However, we think that even though this run is not quantitatively fully comparable to the others, it still illustrates the fact that the qualitative results remain unchanged as a function of resolution.
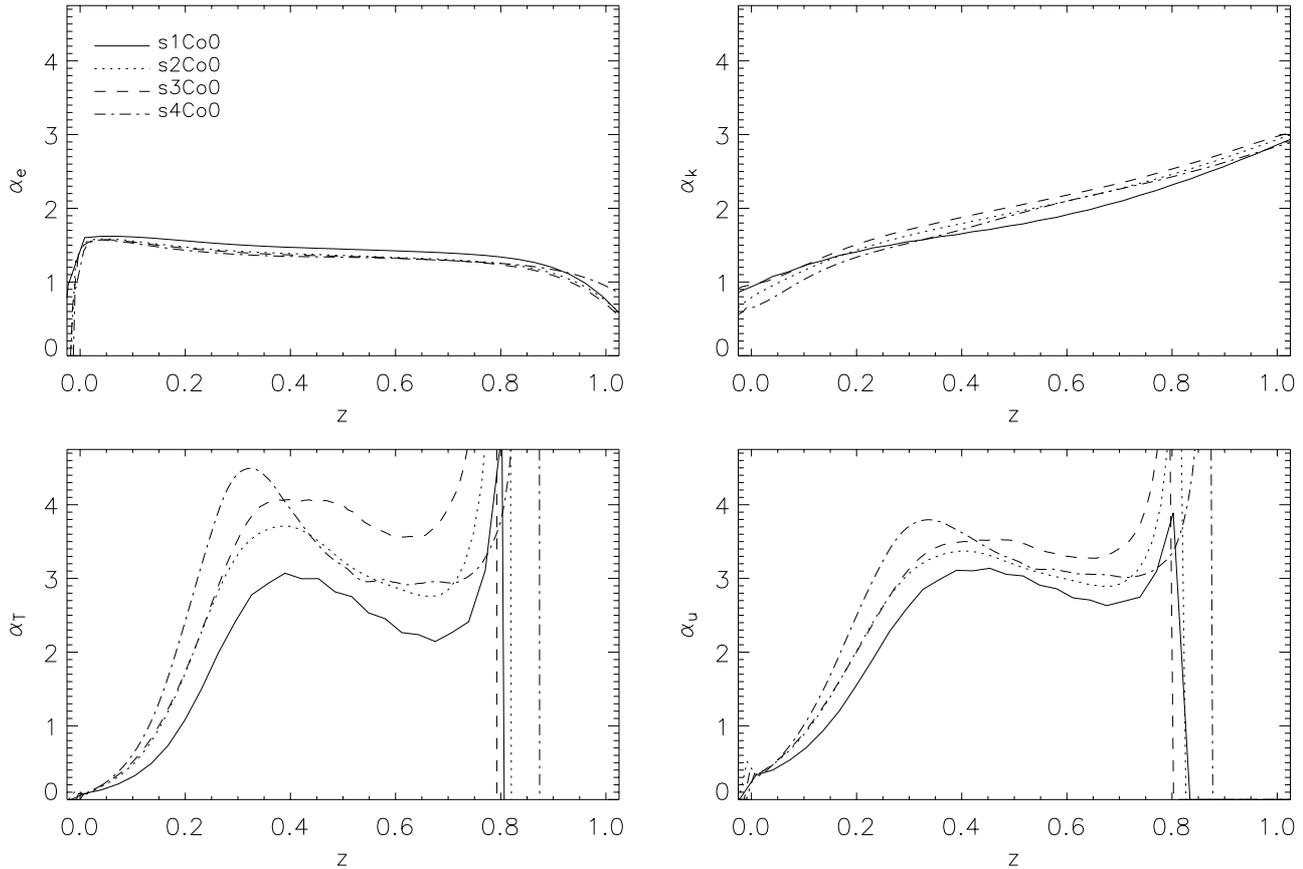
Fig. 8. Mixing length parameters α_i, defined via Eqs. (12) to (15), as function of Ra and resolution for the runs siCo0 from Table 1.

5.4. Application to a solar model

As the Coriolis number in the lower part of the convection zone is large, the convective efficiency should be substantially reduced according to the 3D numerical calculations. In the one-dimensional standard solar model we simulate this by a reduced mixing length. However, there are virtually no consequences to the solar structure *within* the convection zone. This is because the temperature gradient, as determined by mixing-length theory, closely follows the adiabatic gradient, irrespective of the details of the convection formalism.

On the other hand, the overshooting *below* the base of the convection zone may be severely reduced by a reduced convective efficiency. This can be illustrated by solar models that employ a non-local version of the mixing-length formalism (Skaley & Stix 1991; Stix 2002). In those models the temperature excess ΔT and the convection velocity v are determined as integrals over the distance a convection parcel travels in the vertical direction. If this distance is reduced, the parcel acquires less kinetic energy, so that there is less overshooting. In Fig. 9 this is shown for a standard model calculated with local mixing-length theory and two non-local models. We find that the depth of overshooting decreases approximately in proportion to the decrease of the integration path. If the average parcel path is reduced by a factor 2.5, which is consistent with the numerical results, overshooting extends only over $\approx 2900\,\mathrm{km}$.
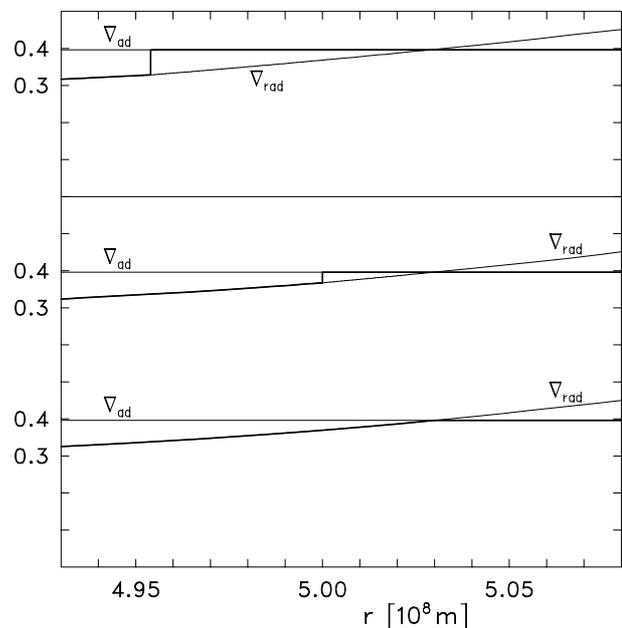

Fig. 9. Temperature gradients $\nabla = d\ln T/d\ln P$ near the base of the convection zone. The actual gradient (*heavy line*) is identical to the radiative gradient in the core, and closely follows the adiabatic in the convection zone and in the region of overshooting. A local model with no overshooting (*lower line*); non-local models with mean path $l/2$ (*above*), as assumed in local theory, and with mean path $l/5$ (*middle*).

Christensen-Dalsgaard et al. (1995) determined an upper limit of $\approx 0.1 H_p$ for overshooting with a sharp transition from the adiabatic to the radiative regime, such as we obtain with the non-local mixing length models. Beyond this limit the discontinuity of the temperature gradient would leave a measurable signature in the spacing of p-mode frequencies. Thus, the rotational quenching of the overshooting would appear to be welcome. On the other hand, the total depth of the convection zone may become too small in this way. The problem is aggravated as a recent redetermination of the abundance of oxygen and other heavy elements (Asplund et al. 2004) lowers the opacity and, therefore, also leads to a shallower convection zone. Bahcall et al. (2005) find $r/r_\odot = 0.726$ for the base of the convection zone of their model BP04+ which incorporates the new lower opacity as well as best available updates of all other input parameters. This means that the convection zone would be too shallow by ≈ 9000 km or $\approx 0.2 H_p$, as compared to the helioseismological result ($r/r_\odot = 0.713 \pm 0.001$; Christensen-Dalsgaard et al. 1991; Basu & Antia 1997).

Presently is is not clear how this conflict will be resolved. New opacity calculations (Seaton & Badnell 2004) yield an increase of 5% compared to the latest OPAL values; but this is only about half the increase needed: Bahcall et al. (2005) obtain a sufficiently deep convection zone if they increase the opacity by $\approx 10\%$ in the depth range $0.4 r_\odot$ to $0.7 r_\odot$. We suggest that the solution is a combination of modest overshooting and a modest opacity increase. Overshooting may also account for the whole difference if it avoids the sharp transition that occurs in our calculation. Rempel (2004) has proposed a model in which the mixing between downflows and upflows is crucial for the total depth of the overshooting, and in which an ensemble of downflows with different strength produces a smooth transition.

References

Asplund, M., Grevesse, N., Sauval, A. J., Allende Prieto, C., & Kiselman, D. 2004, A&A, 417, 751

Bahcall, J. N., Basu, S., Pinsonneault, M., & Serenelli, A. M. 2005, ApJ, 618, 1049

Basu, S., & Antia, H. M. 1997, MNRAS, 287, 189

Basu, S., & Antia, H. M. 2001, MNRAS, 324, 498

Biermann, L. 1932, Z. Astrophys., 5, 117

Böhm-Vitense, E. 1958, Z. Astrophys., 46, 108

Caunt, S. E., & Korpi, M. J. 2001, A&A, 369, 706

Chan, K. L., & Sofia, S. 1987, Science, 235, 465

Chan, K. L., & Sofia, S. 1989, ApJ, 336, 1022

Chan, K. L., & Sofia, S. 1996, ApJ, 466, 372

Christensen-Dalsgaard, J., Gough, D. O., & Thompson, M. J. 1991, ApJ, 378, 413

Christensen-Dalsgaard, J., Monteiro, M. J. P. F. G., & Thompson, M. J. 1995, MNRAS, 276, 283

Cowling, T. G. 1935, MNRAS, 96, 42

Käpylä, P. J., Korpi, M. J., & Tuominen, I. 2004, A&A, 422, 793 (Paper I)

Kim, Y.-C., Fox, P. A., Demarque, P., & Sofia, S. 1996, ApJ, 461, 499

Monteiro, M. J. P. F. G., Christensen-Dalsgaard, J., & Thompson, M. J. 1994, A&A, 283, 247

Prandtl, L. 1925, Z. Angew. Meth. Mech., 5(2), 136

Porter, D. H., & Woodward, P. R. 2000, ApJS, 127, 159

Rempel, M. 2004, ApJ, 607, 1046

Robinson, F. J., Demarque, P., Li, L. H., et al. 2003, MNRAS, 340, 923

Seaton, M. J., & Badnell, N. R. 2004, MNRAS, 354, 457

Skaley, D., & Stix, M. 1991, A&A, 241, 227

Stix, M. 2002, The Sun: An introduction, Second Edition (Berlin, Heidelberg, New York: Springer-Verlag)

Taylor, G. I. 1915, Phil. Trans. R. Soc. London A., 215, 1

Vitense, E. 1953, Z. Astrophys., 32, 135